Science & Technology Development Journal – Engineering and Technology, 4(SI2):SI1-SI11

Open Access Full Text Article

Research Article

Development of a Laminar Air Flow System for Preventing Surgical Equipment Table Infections

Thanh-Long Le[1,2,*], Trung Nghia Tran[2,3], Hoang Kim Son Mai[1,2], Thai Son Tran[2,3]

Use your smartphone to scan this QR code and download this article

ABSTRACT

Nowadays, the infections cause the higher patient mortality and longer time in hospitals and clinical treatment units. It requires the good quality of healthcare services. This paper presents the research in an attempt to realize a mobile laminar airflow system for preventing the contamination of airborne pathogens by protecting the surgical site area as well as the instrument table as low-cost as possible. The portable laminar airflow system and centrifugal fan are modeled by using computer-aided design (CAD) software. This system concludes a blower, UVC lamp, standard filter, high-efficiency particulate air (HEPA) filter, and instrument table. Then, the proposed device was verified through numerical simulations. Computational Fluid Dynamics (CFD) was performed to optimize the system design by examining and evaluating the results, as well as computing the aerodynamic characteristics for the system's centrifugal blower and taking fan pressure variation into account while adjusting inlet flow. As a result, sterile conditions may be created instantaneously and anyplace using this proposed laminar airflow system. The innovative layered airflow sterilizer may achieve a local Biosafety Level II in a specific area, such as an isolation room, patient bedroom, or operating room. After modeling the system, the finer mesh of centrifugal fan was carried out to ensure the accuracy of numerical simulation. There are four domains discretized in a centrifugal fan such as impeller fluid domain, volute fluid domain, inlet, and outlet fluid domain. The inlet mass flow rate strongly affects the performance of the centrifugal fan. The numerical results show that the total pressure maintained inside the blower increase as the flow rate gets larger. The results of this study provide an essential basis for optimizing system design in future investigations.

Key words: Computational Fluid Dynamics, Centrifugal Fan, Air Flow System, Aerodynamic

[1]*Faculty of Mechanical Engineering, Ho Chi Minh City University of Technology (HCMUT), 268 Ly Thuong Kiet Street, District 10, Ho Chi Minh City, Vietnam*

[2]*Vietnam National University Ho Chi Minh City, Linh Trung Ward, Thu Duc City, Ho Chi Minh City, Vietnam*

[3]*Faculty of Applied Science, Ho Chi Minh City University of Technology (HCMUT), 268 Ly Thuong Kiet Street, District 10, Ho Chi Minh City, Vietnam*

Correspondence

Thanh-Long Le, Faculty of Mechanical Engineering, Ho Chi Minh City University of Technology (HCMUT), 268 Ly Thuong Kiet Street, District 10, Ho Chi Minh City, Vietnam

Vietnam National University Ho Chi Minh City, Linh Trung Ward, Thu Duc City, Ho Chi Minh City, Vietnam

Email: ltlong@hcmut.edu.vn

History

- Received: 20-7-2021
- Accepted: 18-8-2021
- Published: 25-8-2021

DOI : 10.32508/stdjet.v4iSI2.877

Check for updates

VNU-HCM Press

I NTRODUCTION

Following the global COVID-19 outbreak, these experts identified signs of the possibility of airborne disease transmission. The COVID-19 has highlighted the possibility of airborne dissemination not only in outdoor and crowded areas but also in indoor environments. In hospitals or clinical treatment units, airborne infection exposure is more frequent and poses greater risks than before [1–5]. The risk of cross-infection from these airborne pathogens is greater in vulnerable hospital patients and the healthcare staff who work for them [6]. Along with that, each medical facility's hospital is raising awareness about the prevention of epidemics and infections. Nosocomial infections, particularly postoperative infections, are common following surgery because of various risk factors that are contributing like age, duration of operation, number of persons within the operation room, the general condition of the operating theatre... The nosocomial infections prolonged the lengths of hospitalization, developed multi-organ dysfunction, and increased mortality. In 1969, Charnley *et al.* [7] found that postoperative infection in orthopedic total hip replacement with prosthetics is closely related to operating room air quality. The improvement of the air cleanliness led to the decline in the rate of wound infection. Li *et al.* [8] also studied the effect of air during a SARS outbreak in a hospital in Hongkong by inspecting the ventilation design and air distribution system. They concluded that it is necessary to improve the quality of the airflow system to reduce the risk of cross-contamination in the isolation ward.

Computational fluid dynamics (CFD) is a well-known technology for solving numerical issues relating to fluid mechanics. Le *et al.* [9–13] used the CFD simulation scheme to evaluate fluid motion and hydrodynamic characteristics (pressure, velocity, etc.) in a microchannel or sterilization chamber. Because of the time and cost savings, CFD is also widely applied in the medical profession in the numerical simulation of infection, pathogen dispersion, and the performance of ventilation systems... Ho [14] and Peng *et al.* [15] presented CFD simulations for evaluating the airborne pathogen transport and transmission risks of the virus. Ho found that wearing a face mask or

Cite this article : Le T, Tran T N, Mai H K S, Tran T S. **Development of a Laminar Air Flow System for Preventing Surgical Equipment Table Infections**. *Sci. Tech. Dev. J. – Engineering and Technology;* 4(SI2):SI1-SI11.

face shield could reduce the risk of disease transmission. Yamakawa *et al.*[16] performed numerical simulations to study the prolonged dispersion of the coronavirus in the classroom. A CFD simulation to precisely analyze the effect of face shields in reducing Coronavirus transmission was performed by Tretiakow *et al.*[17]. Bhattacharyya *et al.*[18] reported a study on the bactericidal effect of air from air-conditioning machines combined with aerosol sanitizer in hospital isolation rooms. Lu *et al.*[19] used CFD to analyze a stratum ventilation system in a hospital for the reduction of exposure risk. Ascione *et al.*[20] have applied CFD in classroom design in the time of COVID-19. Beggs *et al.*[21] performed CFD calculations to evaluate different ventilation strategies in removing airborne pathogens and concluded that airflow plays a significant role in reducing the incidence of infectious diseases, through improving ventilation systems can reduce environmental contamination and nosocomial infection rates in hospital. A dispersion model of infectious pathogens due to human activities in a hospital ventilated space was constructed by Hathway *et al.*[22]. The laminar airflow system provides a wide, secure safety zone around the patient and the surgical team (including their instruments), significantly reducing the risk of germ and airborne particle contamination. Laminar air-flow units are generally two types: ceiling-mounted (vertical flow) or wall-mounted (horizontal flow). They are intended to reduce pollution by delivering a consistent and significant amount of filtered air to the surgical room, and contaminants are washed out immediately. Therefore much attention has been paid to the laminar airflow system in a hospital. Sadrizadeh *et al.*[23] created a model of an operations room using two different ventilation strategies. They came to the conclusion that the horizontal laminar airflow system outperformed the vertical system since the surgical lamps and heat plumes have little impact on horizontal airflow patterns, and the horizontal system is simple to build and operate, cheap and does not necessitate modifications to current surgical lamps or air conditioning systems. However, to have the greatest result of removing infectious diseases, it is always important to pay attention to the actions of humans and other objects. Furthermore, there is a lot of research on mobile laminar airflow systems that are used for a small region in the operation room, such as the instrument table. Lapit-Gortzak *et al.*[24] investigated the anti-infective effectiveness of mobile ultra-clean unidirectional airflow in an intravitreal injection simulation environment. The study revealed that the instrument table has a protection factor of up to 5 and the ocular surface has a protection factor of 2.64 ($p < 0.05$) to 5 ($p < 0.05$), which is possible to eliminate respiratory infections during the intravitreal injection. Reducing contamination efficiency in operating rooms with vertical airflow system and mobile laminar airflow unit was studied by Casagrande *et al.*[25]. The reports emphasize the significance and relevance of assessing the relationship between the mobile laminar airflow unit and the operating room's installed laminar airflow system. The indiscriminate application of mobile laminar units can pose several dangers, diminishing the area's sterility. Sadrizadeh *et al.*[26] concluded that if the primary operating room ventilation system is unable to minimize the degree of microbiological contamination to an acceptable level for orthopedic implant surgery, the MLAF screen unit may be a viable solution. Moreover, CFD is used in the research of aerodynamic characteristics and the optimization of industrial equipment including centrifugal air blowers. Zhou *et al.*[27] optimized centrifugal fan blade design using the Hicks-Hence function and a multi-objective genetic algorithm. Ye *et al.*[28] investigated the performance and flow behaviors of the multi-blade centrifugal fan by the CFD method. Many numerical studies have been performed on the applicability of fixed and mobile laminar airflow systems in hospitals, as well as the aerodynamic characteristics of centrifugal fans, but they are independent and have no effect on each other. A new portable laminar airflow system design with a centrifugal fan as the primary component has been developed. Therefore the laminar airflow unit and the centrifugal fan are inextricably tangled up. The performance of the centrifugal fan influences the efficiency of the airflow system. To assess this design, research must be conducted to evaluate both the aerodynamic characteristics of the centrifugal fan and its influence on the performance of the portable laminar airflow system in the hospital operating room.

In this paper, the numerical study is carried out to analyze the new design of a useful, efficient, and low-cost portable laminar airflow system, the primary component of which is a forward-curved centrifugal fan. Therefore, the model of the centrifugal fan and airflow system was created, and CFD simulation was used to investigate the aerodynamic characteristics of the centrifugal fan, as well as the corresponding influence of the airflow unit on the ventilated area in the hospital operating room.

METHODOLOGY

Portable laminar airflow system design

The model of the laminar airflow system is constructed by using computer-aided design (CAD) software, represent all important features of a real system. This consists of a blower, filter, UVC lamp, high efficiency particulate air (HEPA) filter, and instrument table. This study concentrates on evaluating airflow through the system therefore many solid parts that do not affect the calculation are ignored to simplify the computational process. Figure 1 shows the instrument table with sizes of 500 *mm* x 1000 *mm*. The air filter G4 dimensions are 289 *mm* x 594 *mm* x 46 *mm* for removing the airborne particles > 10 *micrometers* (μm) in diameter. The centrifugal blower 3500 *rpm* offers 620 m^3/h and static pressure *500.0* Pascal *(Pa)*. The HEPA filter H14 dimensions are 610 *mm* x 305 *mm* x 149 *mm*. This HEPA filter removes at least 99.995% of airborne particles 0.3 *pm* in diameter. The minimal resistance of the filter to airflow (pressure drop) is specified around 300 *Pa* (0.044 psi) at its nominal volumetric flow rate.

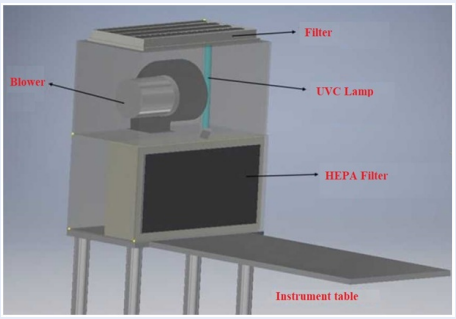

Figure 1: The model device with main components.

In Figure 2, a brief 3D model of the portable laminar airflow system for numerical calculation and space equivalently sized of the instrument table have been established to analyze the effects of the system on the air area around the table and the difference between this air area and the air area in the room.

Air blower design

Centrifugal blowers are widely used in all kinds of engineering applications such as ventilation, processes of air supply, consumer electronics…because of their large mass flow rate and compactness. In this study, a 3D centrifugal blower model was developed using numerical methods for the inspection of flow conditions. The three-dimensional centrifugal fan was first

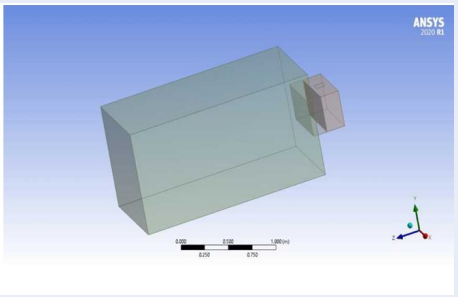

Figure 2: The 3-dimensional model of system.

generated by CAD software, which represents all important features of a real system. The main components of the blower are the impeller, inlet, outlet, and volute. This study concentrates on evaluating the airflow of the blower, therefore many solid parts that do not affect the calculation are ignored to simplify the computational process. The impeller blades are thin, have the same thickness and each profile is a simple arc curve. These important parameters determine the quality of the air blower's internal flow field.

The blade profile varies of impeller could be determined using the tangent circular arc method. The equation of calculating blade profile is written as:

$$P = \frac{R_2^2 - R_1^2}{2\left(R_2 \cos\beta_2 - R_1 \cos\beta_1\right)} \quad (1)$$

where R_2 and R_1 are the impeller outer and inner radius, respectively. Likewise, β_2 and β_1 are the blade outlet and inlet angle, respectively. Figures 3 and 4, and Table 1 show the 3D geometry of the centrifugal fan, impeller, and data of the fan, respectively.

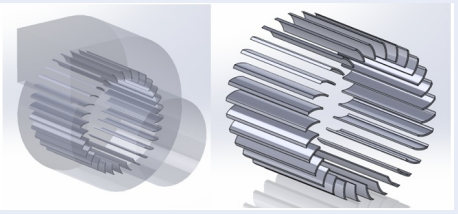

Figure 3: Basic structure of centrifugal fan model.

Numerical approach

The simulation was performed with ANSYS Fluent 2020 software. The Standard perturbation chamber with an inlet particle flow rate of 0.18 *kg/s*. The air passing through the Porous area (which is the space of the HEPA filter) with the laminar type airflow, has

Table 1: Basic parameter of the fan

Fan structure	Dimension
Number of blades	30
Impeller length (mm)	100
Impeller outer radius, R2 (mm)	62
Impeller inner radius, R1 (mm)	50
Blade thickness (mm)	1.2
Blade inlet angle, $\beta 1$ (^{o})	90
Blade outlet angle, $\beta 2$ (^{o})	153
Volute width (mm)	105
Speed of fan (rpm)	3500

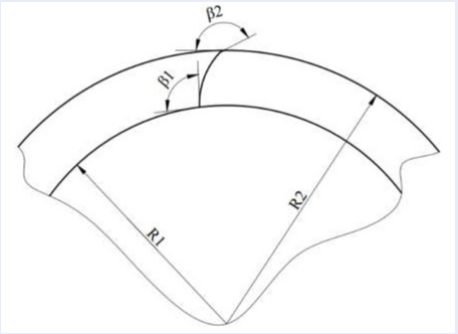

Figure 4: Blade physical model.

a viscous resistance of 1.105x10^8 $1/m^2$ and an inertial resistance of 0.7 $1/m$. The method of implementation is SIMPLE Scheme, Standard Initialization, which is repeated 1000 times to achieve statistically reliable results. ANSYS Fluent 2020 was also used to solve the airflow of the blower. The multi-reference frame (MRF) model was selected to define the relative motion between stationary and rotating parts of the blower. The impeller fluid domain was set as the rotation area with the rotating frame of reference. Meanwhile, the other domains were set as a stationary area in the inertial frame of reference. To simulate the behavior of flow, a CFD solver is set up to find the converged solution of the system of governing equations such as the continuity, momentum equations Reynolds averaged Navier-Stokes equations for compressible flow at constant temperature.

$$\frac{\partial \bar{\rho}}{\partial t} + \frac{\partial}{\partial x_j}\left(\bar{\rho}\widehat{u}_j\right) = 0 \tag{2}$$

$$\frac{\partial\left(\bar{\rho}\widehat{u}_i\right)}{\partial t} + \frac{\partial}{\partial x_j}\left(\bar{\rho}\widehat{u}_j\widehat{u}_i\right) = \frac{\partial p}{\partial x_i} + \frac{\partial \bar{\sigma}_{ij}}{\partial x_j} + \frac{\partial \tau_{ij}}{\partial x_j} \tag{3}$$

$$\begin{aligned}&\frac{\partial\left(\bar{\rho}\widehat{E}\right)}{\partial t} + \frac{\partial}{\partial x_j}\left(\widehat{u}_j\bar{\rho}\widehat{H}\right)\\ &= \frac{\partial p}{\partial x_i}\left(\bar{\sigma}_{ij}\widehat{u}_i + \overline{\sigma_{ij}u_i^{"}}\right)\\ &-\frac{\partial}{\partial x_j}\left(\bar{q}_j + c_p\rho\overline{u_j^{"}T^{"}} - \widehat{u}_i\tau_{ij} + \frac{1}{2}\rho\overline{u_i^{"}u_i^{"}u_j^{"}}\right)\end{aligned} \tag{4}$$

where

$$\widehat{H} = \widehat{E} + \bar{p}/\bar{\rho}$$
$$\bar{q}_j = -\overline{k_T\partial T/\partial x_j} \approx \frac{c_p\widehat{\mu}}{Pr}\frac{\partial\widehat{T}}{\partial x_j}$$

and the viscous stress tensor is

$$\bar{\sigma}_{ij} \approx 2\widehat{\mu}\left(\widehat{S}_{ij} - \frac{1}{3}\frac{\partial\widehat{u}_k}{\partial x_k}\delta_{ij}\right)$$

The reliable k-ε module was used. According to Yoon and Shih *et al.* [29,30], this module is widely used for calculating turbulent flow by solving two transport equations: kinetic energy equation (k) and turbulent dissipation equation (ε). The k-ε model can be realized as it satisfies many of the mathematical constraints applied Reynolds stress. Realization helps to come up with a realistic solution to rotational motion and pressure gradients problems. It helps to achieve better results in solving turbulence problems inside the centrifugal fan. It offers a good compromise between numerical effort and computational accuracy which is very useful in the study and industrial applications.

The kinetic energy equation (k) is described as:

$$\frac{\partial(\rho k)}{\partial t}+\frac{\partial}{\partial x_j}(\rho k u_j) = \frac{\partial}{\partial x_i}\left[\left(\mu+\frac{\mu_t}{\sigma_k}\right)\frac{\partial_k}{\partial x_j}\right] + P_k + P_b - \rho - Y_M + S_k \quad (5)$$

The turbulent dissipation equation (ε) is written as:

$$\frac{\partial\left(\rho \overset{\cdot}{o}\right)}{\partial t}+\frac{\partial}{\partial x_j}\left(\rho \overset{\cdot}{o} u_j\right) = \frac{\partial}{\partial x_i}\left[\left(\mu+\frac{\mu_t}{\overset{\cdot}{\sigma}_o}\right)\frac{\partial \overset{\cdot}{o}}{\partial x_j}\right] + \rho C_1 S \overset{\cdot}{o} - \rho C_2 \frac{\overset{\cdot}{o}^2}{k+\sqrt{\overset{\cdot}{v}o}} + C_{1\overset{\cdot}{o}}\frac{\overset{\cdot}{o}}{k} C_{3\overset{\cdot}{o}} P_b + S \overset{\cdot}{o} \quad (6)$$

where:

$C_1 = max\left[0.43; \frac{\eta}{\eta+5}\right]$;

$\eta = S\frac{k}{\overset{\cdot}{o}}$;

$S = \sqrt{2 S_{ij} S_{ji}}$;

u_j: Velocity component in the corresponding direction

u_t: Eddy viscosity, $u_t = \rho C_\mu \frac{k^2}{\overset{\cdot}{o}}$;

$C_\mu = 0.09$; $\sigma_k = 1$;

$\overset{\cdot}{\sigma}_{o=1.3}; C_{\overset{\cdot}{1o}}=1.44$;

The fluid domain is decomposed into a finite set of control volumes. The conservation equations for mass, momentum, energy, species are solved on this set of finite volumes. The governing equations of the flow of a Newtonian fluid are continuity equation, momentum equations, energy equation, and equation of state. These continuous partial differential equations are discretized into a system of linear algebraic equations which can be solved by ANSYS software. The discretized solutions for a CFD problem velocity, pressure, temperature, volume fraction, etc., are distributed on the model.

After modeling the system, the meshing was carried out. Four fluid domains were discretized: impeller fluid domain, volute fluid domain, inlet, and outlet fluid domain. The second-order upwind difference scheme is used for the spatial discretization of the convection terms. The pressure–velocity coupling is deal with a SIMPLE algorithm. After generation, the mesh was carried out in Figure 5. There are 4264 nodes and 3632 elements in the computational model.

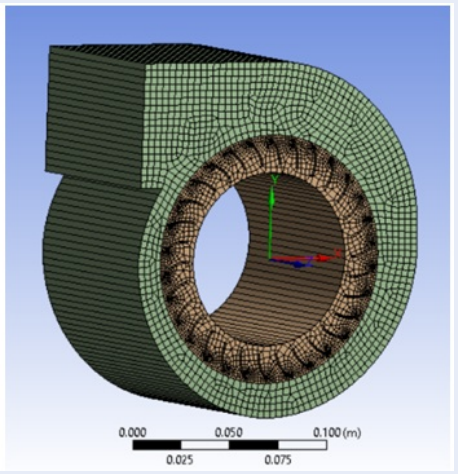

Figure 5: Meshed centrifugal fan.

RESULTS AND DISCUSSION

Figure 6 visualizes the distribution of pressure distributions inside the laminar airflow system. From the center to the housing, the pressure field increases in magnitude. The highest pressure value located at the outflow of the laminar airflow system air stream is 218.4 Pa. It requires greater pressure to repel pathogens in the afflicted region. The lowest pressure value located at the center of the mobile laminar airflow system is 131.5 Pa.

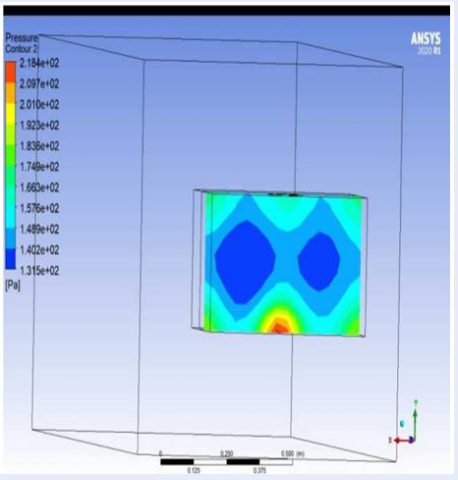

Figure 6: The pressure distribution inside the system.

Figure 7 visualizes the velocity distribution on 04 vertical planes with distances to the HEPA are 100.0 mm, 400.0 mm, 700.0 mm, and 1,000.0 mm, respectively.

The downward airflow from the laminar airflow system is impaired. As one moves away from the air entrance, the velocity of the airflow decreases. The zone of space with high gas velocities and pressure steadily lessens as one moves away from the mobile laminar airflow system. The high-velocity field is extensively spread over the affected region at a distance of 100mm from the HEPA filter, reaching its maximum value sin space near the system outlet. The highest velocity value has dropped at a distance of 400 mm from the HEPA, the high-velocity field is smaller than previously, and there are indicators that the air from the airflow system is dispersing more broadly around. This is the same at 700 mm from the HEPA filter. The high-velocity zone continues to narrow, and the air becomes more widely spread. The high-velocity field of the air narrows to a small region at a distance of 1000 mm from the system, while continuing to scatter more broadly surrounding. As a result, this mobile laminar airflow system will be appropriate for establishing clean air zones for an instrument table with a length of 1000 mm or fewer.

Figure 8 visualizes the velocity distribution in vector at the horizontal middle plane. The characteristics of the gas flow are particularly obvious when viewed in cross-section. The system outlet site has the highest air velocity. The velocity of the air stream tends to decrease as it moves away. The velocity of the airflow directly in front of the outlet is always the greatest and diminishes to the sides. The difference in velocity and pressure of the airflow is a fundamental factor that impacts the ability to create a clean air region for medical instruments on the table, particularly in the operating room. Pathogens in the air tends to flow from the high-pressure area to the low-pressure area, where they are eliminated by the room filtration system. Infectious organisms in the surrounding air are unable to reach the high-pressure region formed by the mobile laminar airflow system. This will aid in the sterilization of the tools, assuring patient safety. Figure 9 depicts the static pressure and velocity contours of an air blower as the impeller rotates at 3500 revolutions per minute. It was discovered that the low-velocity zones are flowing away from the fan center, while the high flow velocity is clearly near the impeller outlet, which is produced by the volute's asymmetry. At the center of the volute, the airflow velocity may reach a maximum of 54.96 m/s. The airstream enters the impeller axially and flows out due to centrifugal force. Furthermore, the pressure value increases from the inlet to the outlet of the centrifugal fan, reaching a maximum of 230.4 Pa at the fan wall.

The flow rate and total pressures are 2.4259 kg/s and 1365.5 Pa, respectively while the fan operates at 3500 revs/min. To gain a more in-depth assessment of the aerodynamic characteristics, particularly how a change in intake flow influences fan total pressure, this study investigated the correlation of inlet mass flow rate with the fan total pressure, as shown in Figure 10. As the results show, there is no doubt that a higher inlet flow rate results in a higher total pressure value. These two quantities have an almost proportional relationship. This is a logical result since a high input flow, which corresponds to a stronger fan suction, will increase in pressure parameters in the fan.

To investigate the aerodynamic characteristics of this forward-curved centrifugal fan in greater depth, the mass flow rate behavior of the fan illustrated in Figure 11 at three different rotational speeds for 5 seconds is the objective of this investigation. As can be seen from the results, there is no doubt that a greater speed means greater suction, resulting in a larger inflow of air. The inlet mass flows of the blower approximately 2.67, 2.43, and 2.32 kg/s corresponding to the rotational speed of 3700, 3500, and 3400 revs/min. The mass flow rate line demonstrates consistency at each speed value.

Figure 12 compares the max total pressure values in five seconds of the fan at three different rotational speeds. The graph shows that a larger rotational speed will result in a larger max total pressure value. When operating at speeds of 3700, 3500, and 3400 revs/min, the centrifugal maximum total pressure values are approximately 1723.8 Pa, 1365.5 Pa, and 1308.8 Pa, respectively. There are three stages to pressure development through a centrifugal fan impeller. At the first stage, the airflow is straight to the surface of the blades. The impellers split the air into small volumes. Here the accumulation of air mass occurs, that is the compression of the air mass of small volume. At the second stage, the air pressure is pumped inside the working chamber. The relative velocity reduces as the air flows through the blade passage, leading to an additional increase in static pressure and dynamic pressure at the impeller outlet. At the final stage, the compressed air is discharged from the working chamber to the outlet. As the air moves radially through the impeller, the absolute velocity of the flow will increase, with the maximum absolute velocity at the impeller outlet. This increase in the absolute velocity of the air leads to an increase in the kinetic energy and dynamic pressure across the impeller. This three stages process creates a repetitive up and down movement in the max total pressure and mass flow rate diagrams in Figure 11 and Figure 12.

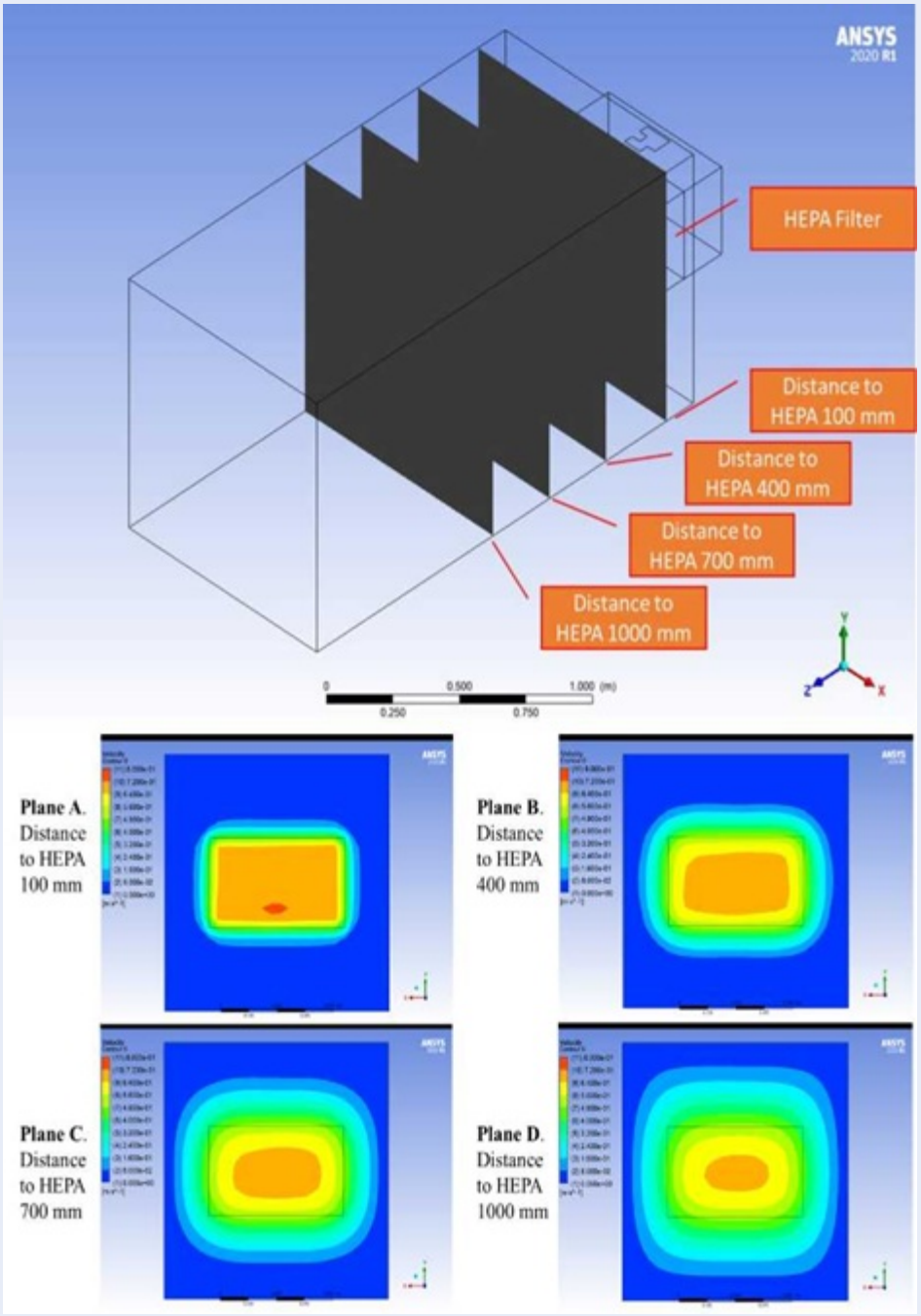

Figure 7: The velocity distribution on 4 planes with distances to the HEPA are 100.0 mm, 400.0 mm, 700.0 mm, and 1,000.0 mm, respectively.

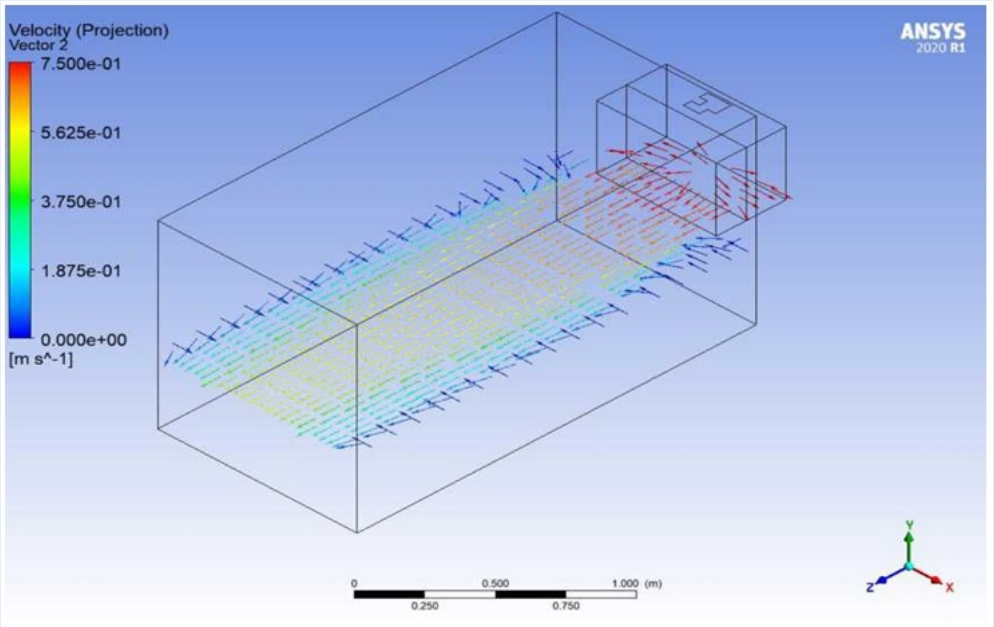

Figure 8: The velocity distribution in vector at the middle plane.

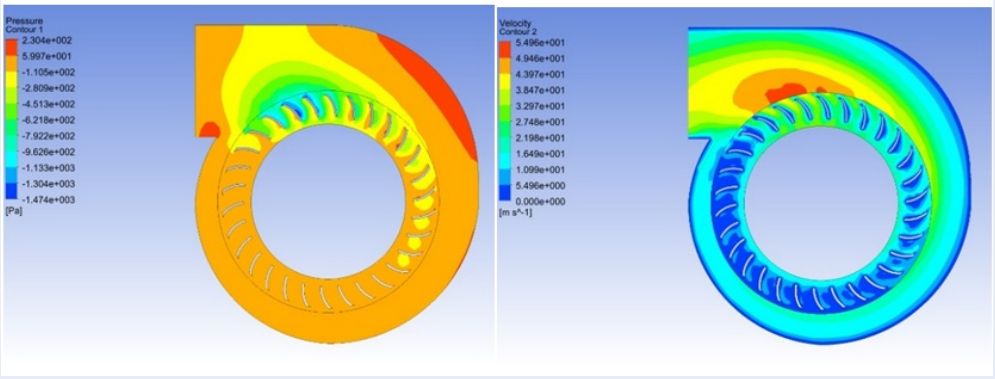

Figure 9: Pressure contour and velocity contour of fan at the speed of 3500 revs/min.

CONCLUSIONS

With the view towards the realization of a portable laminar airflow system to reduce the airborne pathogen dispersion, a novel device was proposed and designed. The computational fluid dynamics method was used to simulate the airflow with pressure and velocity distribution in the laminar airflow system. The results show that this portable laminar airflow system has created a large pressure space, thus creating a clean air area for the instrument table, thereby repelling infectious bacteria present in the operating room air from the ventilated area. The centrifugal blower has been modeled, meshed, and analyzed to study the characteristics of the flow field such as pressure and velocity distribution. Moreover, by changing the input parameter, the effect of different inlet flow rates on the performance of a centrifugal fan such as total pressure was studied by CFD simulations. The numerical results show that the inlet mass flow rate has a great influence on the performance of the fan. The total pressure maintained inside the blower increase as the flow rate gets larger. The figures obtained from numerical results give the potential to upgrade and optimize the new design of the portable laminar airflow system in further studies. With the development of the computational method, the flow patterns of air inside

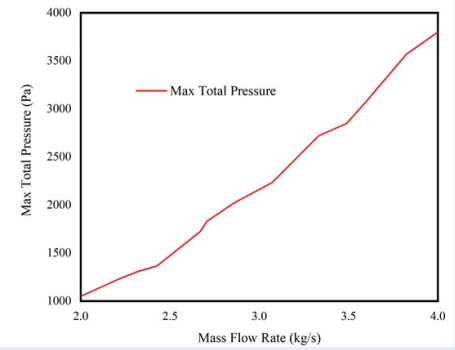

Figure 10: Relationship between Mass Flow Rate (Kg/s) and Max Total Pressure (Pa) of the centrifugal blower.

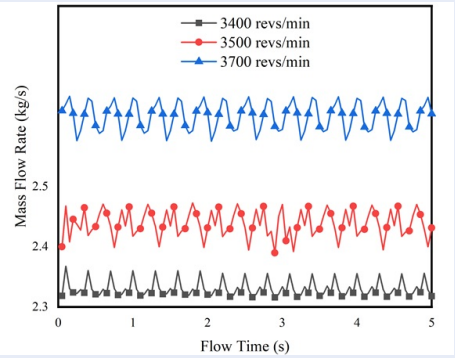

Figure 11: Mass flow rate of the fan at three different rotational velocity in 5 seconds.

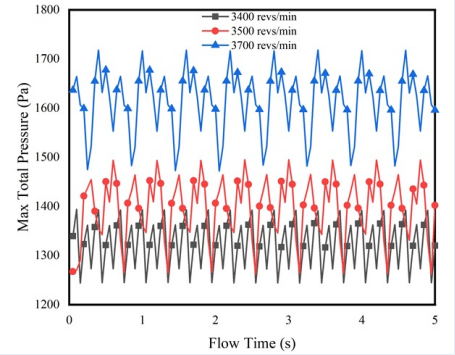

Figure 12: Max total pressure of the fan at three different rotational velocity in 5 seconds.

the blower are analyzed, which will help in a better understanding of the flow behavior of the centrifugal fan. Therefore, the number of experiments also reduced. It will help to reduce cost and lead time for any new design air blower and laminar airflow unit studies. Through this research, the feasibility and the effectiveness of the proposed device were confirmed by the CFD simulation. With the results in this study, the prototype device shall be fabricated and verified by the experiments in further study.

ABBREVIATIONS

CAD: Computer-aided Design
CFD: Computational Fluid Dynamics
HEPA: High Efficiency Particulate Air
MRF: Multi-reference Frame

CONFLICT OF INTEREST

The authors wish to confirm that there are no know conflicts of interest associated with this publication and there has been no significant financial support for this work that could have influenced its outcome.

AUTHORS' CONTRIBUTION

All authors conceived of the study and participated in its design and coordination and helped to draft the manuscript. The authors read and approved the final manuscript.

ACKNOWLEDGEMENT

We acknowledge the support of time and facilities from Ho Chi Minh City University of Technology (HCMUT), VNU-HCM for this study.

REFERENCES

1. Wong TW, et al. Parashar, Outbreak Study Group, Cluster of SARS among medical students exposed to single patient, Hong Kong, Emerging Infectious Diseases 10 (2004) 269-276;Available from: https://doi.org/10.3201/eid1002.030452.
2. Yu ITS, et al. Evidence of airborne transmission of the severe acute respiratory syndrome virus, New England Journal Medicine 350 (2004) 1731-1739;Available from: https://doi.org/10.1056/NEJMoa032867.
3. Dawood FS, et al. Emergence of a novel swine-origin influenza A (H1N1) virus in humans, New England Journal of Medicine 360 (2009) 2605-2615;Available from: https://doi.org/10.1056/NEJMoa0903810.
4. Smith GJ, et al. Dating the emergence of pandemic influenza viruses. Proceedings of the National Academy of Sciences of the USA 106 (2009) 11709-11712;Available from: https://doi.org/10.1073/pnas.0904991106.
5. Tang JW, et al. Ridgway, Factors involved in the aerosol transmission of infection and control of ventilation in healthcare premises, Journal of Hospital Infection 64 (2006) 100¬114;Available from: https://doi.org/10.1016/j.jhin.2006.05.022.
6. Wong BCK, et al. Possible role of aerosol transmission in a hospital outbreak of influenza, Clinical Infectious Diseases 51 (2010) 1176-1183;Available from: https://doi.org/10.1086/656743.
7. Charnley J, et al. Postoperative infection in total prosthetic replacement arthroplasty of the hip-joint with special reference to the bacterial content of the air of the operating room, British Journal of Surgery 56(9) (1969) 641-649;Available from: https://doi.org/10.1002/bjs.1800560902.
8. Li Y, et al. Role of air distribution in SARS transmission during the largest nosocomial outbreak in Hong Kong, Indoor Air 15(2) (2005) 83-95;Available from: https://doi.org/10.1111/j.1600-0668.2004.00317.x.
9. Le TL, et al. Numerical investigation of the thermocapillary actuation behavior of a droplet in a microchannel, Int. J. Heat Mass Transfer 83 (2015) 721-730;Available from: https://doi.org/10.1016/j.ijheatmasstransfer.2014.12.056.
10. Le TL, et al. Numerical study of the migration of a silicone plug inside a capillary tube subjected to an unsteady wall temperature gradient, Int. J. Heat Mass Transfer 97 (2016) 439-449;Available from: https://doi.org/10.1016/j.ijheatmasstransfer.2015.11.098.
11. Le TL, et al. Numerical study of the thermocapillary droplet migration in a microchannel under a blocking effect from the heated wall, Appl. Thermal Eng. 122 (2017) 820-830;Available from: https://doi.org/10.1016/j.applthermaleng.2017.04.073.
12. Le TL, et al. Numerical investigation of the forward and backward thermocapillary motion of a water droplet in a microchannel by two periodically activated heat sources, Numerical Heat Transfer, Part A: Applications 79(2) (2021) 146-162;Available from: https://doi.org/10.1080/10407782.2020.1814603.
13. Le TL, et al. A CFD study on hydraulic and disinfection efficiencies of the body sterilization chamber, Annals of the Romanian Society for Cell Biology 25(2) (2021) 3998-4004;.
14. Ho CK. Modeling airborne pathogen transport and transmission risks of SARS-CoV-2, Applied Mathematical Modelling 95 (2021) 297-319;Available from: https://doi.org/10.1016/j.apm.2021.02.018.
15. Peng S, et al. The role of computational fluid dynamics tools on investigation of pathogen transmission: Prevention and control, Science of The Total Environment 746 (2020) 142090;Available from: https://doi.org/10.1016/j.scitotenv.2020.142090.
16. Yamakawa M, et al. Computational investigation of prolonged airborne dispersion of novel coronavirus-laden droplets, Journal of Aerosol Science 155 (2021) 105769;Available from: https://doi.org/10.1016/j.jaerosci.2021.105769.
17. Tretiakow D, et al. Mitigation effect of face shield to reduce SARS-CoV-2 airborne transmission risk: Preliminary simulations based on computed tomography, Environment Research 198 (2021) 111229;Available from: https://doi.org/10.1016/j.envres.2021.111229.
18. Bhattacharyya S, et al. A novel CFD analysis to minimize the spread of COVID-19 virus in hospital isolation room, Chaos, Solitons and Fractals 193 (2020) 110294;Available from: https://doi.org/10.1016/j.chaos.2020.110294.
19. Lu Y, et al. Reducing the exposure risk in hospital wards by applying stratum ventilation system, Building and Environment 183 (2020) 107204;Available from: https://doi.org/10.1016/j.buildenv.2020.107204.
20. Ascione F. The design of safe classrooms of educational buildings for facing contagions and transmission of diseases: A novel approach combining audits, calibrated energy models, building performance (BPS) and computational fluid dynamic (CFD) simulations, Energy and Buildings 230 (2021) 110533;Available from: https://doi.org/10.1016/j.enbuild.2020.110533.
21. Beggs CB, et al. The ventilation of multiple-bed hospital wards: review and analysis, American Journal of Infection Control 36(4) (2008) 250-259;.
22. Hathway EA, et al. CFD simulation of airborne pathogen transport due to human activities, Building and Environment 46(12) (2011) 2500-2511;Available from: https://doi.org/10.1016/j.buildenv.2011.06.001.
23. Sadrizadeh S, et al. A numerical investigation of vertical and horizontal laminar airflow ventilation in an operating room, Building and Environment 82(1) (2014) 517-525;Available from: https://doi.org/10.1016/j.buildenv.2014.09.013.
24. Lapid-Gortzak R, et al. Mobile ultra-clean unidirectional airflow screen reduces air contamination in a simulated setting for intra-vitreal injection, International Ophthalmology 37 (2017) 131-137;Available from: https://doi.org/10.1007/s10792-016-0236-1.
25. Casagrande D, et al. Conflicting effects of a portable ultra-clean airflow unit on the sterility of operating rooms: A numerical investigation, Building and Environment 171 (2020) 106643;Available from: https://doi.org/10.1016/j.buildenv.2020.106643.
26. Sadrizadeh S, et al. Does a mobile laminar airflow screen reduce bacterial contamination in the operating room? A numerical study using computational fluid dynamics technique, Patient Safety in Surgery 8 (2014) 27;Available from: https://doi.org/10.1186/1754-9493-8-27.
27. Zhou SQ, et al. Research on blade design method of multi-blade centrifugal fan for building efficient ventilation based on Hicks-Henne function, Sustainable Energy Technologies and Assessments 43 (2021) 100971;Available from: https://doi.org/10.1016/j.seta.2020.100971.
28. Ye JJ, et al. Investigation of the performance and flow behaviors of the Multi-blade Centrifugal Fan based on the Computer Simulation Technology, Wireless Personal Communications 103 (2018) 563-574;Available from: https://doi.org/10.1007/s11277-018-5461-7.
29. Yoon GH. Topology optimization method with finite elements based on the k-ε turbulence model, Computer Methods in Applied Mechanics and Engineering 361 (2020) 112784;Available from: https://doi.org/10.1016/j.cma.2019.112784.
30. Shih TH, et al. A new k- ε eddy viscosity model for high Reynolds number turbulent flows, Computers and Fluids 24(3) (1995), 227-238;Available from: https://doi.org/10.1016/0045-7930(94)00032-T.

Tạp chí Phát triển Khoa học và Công nghệ – Kĩ thuật và Công nghệ, 4(SI2):SI1-SI11

Open Access Full Text Article

Bài nghiên cứu

Phát triển hệ thống luồng không khí để ngăn ngừa nhiễm khuẩn bàn phẫu thuật

Lê Thanh Long[1,2,*], Trần Trung Nghĩa[2,3], Mai Hoàng Kim Sơn[1,2], Trần Thái Sơn[2,3]

TÓM TẮT

Ngày nay, các bệnh nhiễm trùng gây ra tỉ lệ tử vong cho bệnh nhân cao và thời gian nằm viện dài trong các bệnh viện và các cơ sở điều trị lâm sàng. Điều này đòi hỏi chất lượng tốt của các dịch vụ chăm sóc sức khỏe. Bài báo trình bày một nghiên cứu về việc hoàn thiện một hệ thống luồng không khí di động để ngăn ngừa sự ô nhiễm của các mầm bệnh bằng cách bảo vệ vùng dành cho phẫu thuật cũng như bàn dụng cụ với chi phí thấp nhất có thể. Hệ thống luồng không khí di động và quạt ly tâm được mô hình hóa bằng cách sử dụng phần mềm thiết kế có sự hỗ trợ của máy tính (CAD). Hệ thống này bao gồm một quạt gió, đèn UVC, bộ lọc tiêu chuẩn, bộ lọc không khí hiệu quả cao (HEPA) và bàn thiết bị. Thiết bị đề xuất sau đó được kiểm chứng thông qua mô phỏng số. Phương pháp tính toán động lực học chất lưu (CFD) được sử dụng để tối ưu hóa thiết kế hệ thống bằng cách kiểm tra và đánh giá kết quả cũng như tính toán đặc tính khí động học của hệ thống quạt gió ly tâm. Do đó, các điều kiện khử khuẩn có thể được tạo ra ngay tức thì và ở bất kỳ đâu bằng cách sử dụng hệ thống luồng không khí được đề xuất trong nghiên cứu này. Thiết bị khử trùng luồng không khí phân lớp cải tiến có thể đạt được cấp độ an toàn sinh học II cục bộ trong một khu vực cụ thể như phòng cách ly, phòng ngủ của bệnh nhân hoặc phòng phẫu thuật. Sau khi mô hình hóa hệ thống, chúng ta tiến hành chia lưới mịn cho quạt ly tâm để đảm bảo độ chính xác của mô phỏng số. Có 4 miền riêng biệt được chia lưới trong quạt ly tâm gồm miền lưu chất quanh cánh quạt, miền lưu chất dễ hóa hơi, miền lưu chất đầu vào và đầu ra. Lưu lượng dòng không khí vào ảnh hưởng lớn đến hiệu suất của quạt ly tâm. Kết quả mô phỏng số cho thấy áp suất tổng duy trì bên trong quạt gió tăng lên khi tốc độ dòng lưu chất lớn. Kết quả nghiên cứu cung cấp cơ sở khoa học để tối ưu hóa thiết kế hệ thống luồng không khí cho khu vực phẫu thuật trong tương lai.

Từ khoá: Tính toán động lực học chất lưu, Quạt ly tâm, Hệ thống luồng không khí, Khí động lực học

[1]*Khoa Cơ khí, Trường Đại học Bách Khoa Tp.HCM, Việt Nam*

[2]*Đại học Quốc gia Thành phố Hồ Chí Minh, Việt Nam*

[3]*Khoa Khoa học Ứng dụng, Trường Đại học Bách Khoa Tp.HCM, Việt Nam*

Liên hệ

Lê Thanh Long, Khoa Cơ khí, Trường Đại học Bách Khoa Tp.HCM, Việt Nam

Đại học Quốc gia Thành phố Hồ Chí Minh, Việt Nam

Email: ltlong@hcmut.edu.vn

Lịch sử

- Ngày nhận: 20-7-2021
- Ngày chấp nhận: 18-8-2021
- Ngày đăng: 25-8-2021

DOI : 10.32508/stdjet.v4iSI2.877

Check for updates

VNU-HCM Press

Trích dẫn bài báo này: Long L T, Nghĩa T T, Sơn M H K, Sơn T T. **Phát triển hệ thống luồng không khí để ngăn ngừa nhiễm khuẩn bàn phẫu thuật**. *Sci. Tech. Dev. J. - Eng. Tech.;* 5(SI2):SI1-SI11.